



Inhibitory effect of *Eucalyptus* and *Lippia Alba* essential oils on the corrosion of mild steel in hydrochloric acid

Andrés F. Gualdrón ^{*1}, Erika N. Becerra ¹, Dario Y. Peña ¹,
José C. Gutiérrez ², Haydée Q. Becerra ³

¹ Grupo de Investigaciones en Corrosión, Universidad Industrial de Santander, Guatiguará Km 7 Santander, Colombia.

² Laboratorio de Química Industrial, Universidad Industrial de Santander, Bucaramanga, AA 678, Colombia

³ Instituto Colombiano del petróleo, Ecopetrol S.A, Km 7 autopista a Piedecuesta, Santander, Colombia.

Received 28 Aug 2012, Revised 20 Sept 2012, Accepted 20 Sept 2012.

*Corresponding author. andresgualdron_105@hotmail.com, Mob: +57 3173018615, Phone:+576401973

Abstract

The inhibitory effect of two essential oils, Eucalyptus and Lippia Alba, were estimated on the corrosion of mild steel in 0.5 M hydrochloric acid (HCl) using weight loss, Electrochemical Impedance Spectroscopy (EIS) and Tafel polarization curves. Inhibition was found to increase with increasing concentration of the essential oils. The effect of temperature on the corrosion behavior of mild steel in 0.5M HCl with addition of essential oils was also studied. Values of inhibition efficiency calculated from weight loss, Tafel polarization curves, and EIS are in good agreement. Polarization curves showed that Eucalyptus and Lippia Alba essential oils behave as mixed type inhibitors in hydrochloric acid. The results obtained showed that the Eucalyptus and Lippia Alba essentials oils could serve as an effective inhibitor of the corrosion of mild steel in Hydrochloric acid solution. The superficial analysis of mild steel was performed using optical microscopy and infrared spectroscopy.

Keywords: corrosion inhibition, Eucalyptus oil, Lippia Alba oil, electrochemical system, mild steel.

1. Introduction

The corrosion control and prevention of metallic materials in environments such as oils industries, represents a very important and fundamental problem. This is due to industrial environments contain agents highly assets for corrosion as the hydrogen sulfide, carbon dioxide, hydrochloric acid in large proportion, among others. This diversity of agents causes a great complexity of the corrosion process of metallic materials in these environments. Actually, natural coatings are used as barriers against the spread of the oxidizing agents, isolating the metal and preventing its accumulation on the surface (1,2). However, the paintings are degraded; they also suffer oxidation processes and usually they need, perhaps more frequently than other methods, inspection and maintenance plans (3-7).

The use of these natural products such as extracted compounds from leaves or seeds as corrosion inhibitors have been widely re-ported by several authors. Gunasekaran (6) et al. studied the corrosion inhibition of steel by eco-friendly *Zenthoxylum alatum* plant extract in HCl as well as in phosphoric acid medium. Essential oils and leaves extracts are used as common corrosion inhibitors. The anticorrosion activity of leaves extracts as *Murraya koenigi* (7), *Emblca officianilis* (8), *Terminalia chebula* (9), *Sapindus trifolianus* (10), and *Accacia conicianna* (11) was investigated. Corrosion inhibition has also been studied for the essential oils and extracts of *lawsonia* (12). Similar results were also shown by *Rosmarinous officinalis* (13), *Annonas quamosa* (14), *Acacia Arabica* (15), *Carica papaya* (16), *Azadirachta indica* and *Vernonia amydalina* which were used for

steel in acid media. *Nypafructicans wurmb* leaves were studied for the corrosion inhibition of mild steel in HCl media (17-19).

This study is part of the research line in additives of the Instituto Colombiano del Petróleo (ICP), together with the Grupo de Investigaciones en Corrosion (GIC) was carried out to find two several essential oils (*Eucalyptus* and *Lippia Alba*), of easy acquisition and substantially compatible with the environment, which can be used for the inhibition of mild steel in hydrochloric acid solution.

2. Experimental section

2.1. Characterization and chemical composition of essential oils

The chemical components of *Eucalyptus* and *Lippia Alba* essential oils were determined by spectral analysis of gas chromatography coupled to mass spectrometry (GC-MS), in Centro Nacional de Investigaciones Para la Agroindustrialización de Especies Vegetales Medicinales Tropicales (CENIVAM), being identified six major components for each essential oil studied (20,21).

2.2 Mild steel samples preparation

All studies were carried out using Mild Steel (MS) samples of composition, Fe = 99.80% and C = 0.20%. MS samples of size 1.0 x 1.0x 1.0 cm and MS powder were used for weight loss and IR spectroscopy studies respectively. For optical microscopy and electrochemical studies, specimens with an exposed area of 1 cm² were used. These specimens were degreased ultrasonically with 2-propanol and polished mechanically with different grades of emery paper to obtain very smooth surface (22).

2.2. Solutions preparation

The solution 0.5M HCl was prepared by dilution of analytical grade Merck 37% HCl with double distilled water. The test solutions were freshly prepared before each experiment by adding the oil directly to the corrosive solution. Experiments were carried out in triplicate to ensure the reproducibility. The essential oils concentrations were 1.0, 4.0 y 5.0 g/L.

2.3. Weight loss studies

Previously degreased, polished and weighed mild steel samples were immersed in 250 ml test solutions with and without inhibitor concentration 5.0 g/L for each essential oil studied. In order to investigate the effects of temperature on the inhibitor performance, the gravimetric measurements were carried out for a period of four hours at three different temperatures: 298 K, 333 K and 383 K.

2.4. Electrochemical measurements

Electrochemical studies were made using a potentiostat Gill AC BI-STAT ACM instruments piloted by ACM Instruments software. This potentiostat was connected to a conventional three-electrode cell assembly. A saturated calomel electrode (SCE) and graphite electrode were used as reference and auxiliary electrodes, respectively. The material used for constructing the working electrode was the same used for gravimetric measurements. The surface area exposed to the electrolyte was 1 cm² (23,24). Prior to the electrochemical measurement, a stabilization period of 30 minutes was allowed, which was proved to be sufficient to attain a stable value of corrosion potential (E_{corr}).

Tafel polarization curves were plotted at a polarization scan rate of 0.2 mV/s. The polarization curves were obtained by changing the electrode potential automatically from -250 mV to 250 mV vs E_{corr} at 298 K. Anodic and cathodic curve slopes were extrapolated to corrosion potential, for the determination of the corrosion current densities (I_{corr}) (24). The electrochemical impedance spectroscopy (EIS) measurements were carried out in a frequency range from 30 KHz to 0.01 Hz with amplitude of 10 mV value peak by peak, using AC signal as corrosion potential (E_{Corr}). The impedance diagrams are given in the Nyquist representation. Experiments are repeated three times to ensure the reproducibility. All electrochemical studies were carried out with immersion time of 1 hour, with inhibitor concentrations of 1.0, 4.0 and 5.0 g/L, at 298 K (25).

2.5. Fourier Transform Infrared Spectroscopy (FTIR)

Infrared Spectra were recorded in a spectrophotometer Bruker FTIR model Tensor 27 in a frequency range from 4000 cm^{-1} to 500 cm^{-1} . MS specimens with exposure area of 1 cm^2 were prepared as it mentioned above. The metal samples were removed of corrosive solution 0.5M HCl, after an immersion time of 4 h containing 5.0 g/L of inhibitor. The specimens were washed with water distilled and then dried. Subsequently, part of the protective layer adhered on the surface of material was removed, forming with KBr, the corresponding pill to obtain the infrared spectrum of powdered MS specimen (26-29). Furthermore, infrared spectroscopy was used to obtain the IR spectra of Eucalyptus and Lippia Alba essential oils for subsequent comparisons.

2.6. Optical microscopy

The photographs were obtained and recorded in an optical microscope Olympus model Optik. The exposure area of metal specimens with and without inhibitor concentration 5.0 g/L for each essential oil analyzed was observed with a image resolution 100 x, After 4 h of immersion in 250 mL of 0.5M HCl containing 5.0 g/L of each essential oil studied. Also the material surface was observed before the corrosion tests start. (30-37).

3. Results and Discussion

3.1. Essential oil composition

The major components of Eucalyptus and Lippia Alba oil are shown in Table 1 and 2

Table 1. Major chemical constituents of Eucalyptus oil (%)

Nº	Components	%
1	Citronellal	43.00
2	Citronellol	13.0
3	Isopulegol	10.0
4	linalool	4.40
5	1,8-Cineole	4.00
6	β -pinene	3.00

Table 2. Major chemical constituents of Lippia Alba oil (%)

Nº	Components	%
1	Carvona	53.00
2	Biciclosesquifelandrene	16.40
3	limonene	11.10
4	Piperitenone	3.60
5	Piperitone	2.50
6	β -Bourboneno	1.50

3.2. Electrochemical impedance measurements

The corrosion behaviour of mild steel in 0.5M HCl solution, in the absence and presence of Eucalyptus and Lippia Alba essential oils, was investigated by the EIS at 298 K after 1 hour of immersion. The charge-transfer resistance values were obtained from the diameter of the semicircles of the Nyquist diagrams. The inhibition efficiency (E %) of the inhibitor has been found out from the charge transfer resistance values using the following equation:

$$E(\%) = \frac{R_{corr}^o - R_{corr}}{R_{corr}^o} \times 100 \quad (1)$$

where, R_{ct}^o and R_{ct} are the charge transfer resistance in presence and in absence of inhibitors, respectively. All electrochemical measurements were done in unstirred and non de aerated solutions. The electrochemical impedance plots for mild steel in 0.5M HCl solution in the absence and presence of various concentrations of aqueous essential oil from Eucalyptus and Lippia Alba are shown in Figure 1 and 2. Table 3 and 4 summarizes impedance data from the EIS experiments carried out both in the absence and presence of increasing essential oil concentrations.

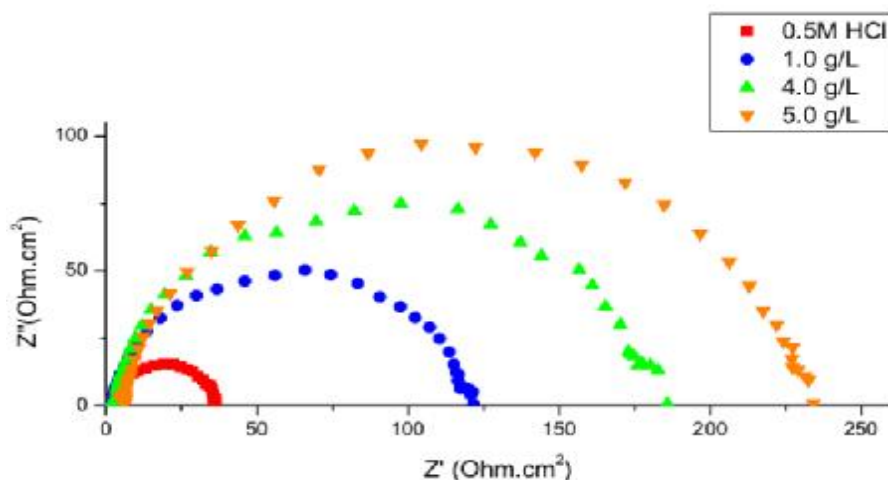


Figure 1. Nyquist plots in absence and presence of different concentrations of Eucalyptus oil in 0.5M HCl

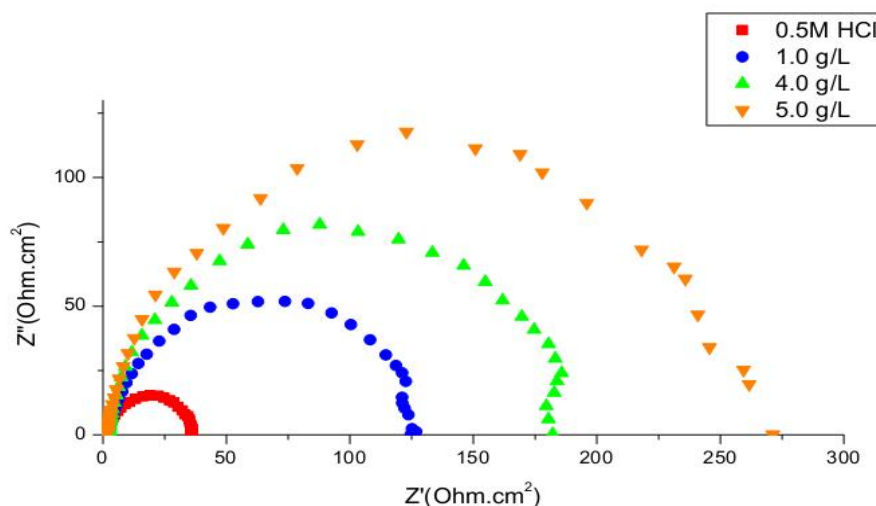


Figure 2. Nyquist plots in absence and presence of different concentrations of Lippia Alba oil in 0.5M HCl

Table 3. Corrosion parameters obtained by impedance measurements for mild steel in 0.5M HCl at various concentrations of Eucalyptus oil.

Inhibitor concentration	R_{ct} (ohm.cm ²)	f_{max} (Hz)	C_{dl} (mF/cm ²)	E (%)
0.5M HCl	36.1	0.35	12.596	-
1.0 g/L	125.7	0.18	7.034	70.3
4.0 g/L	185.8	0.18	4.758	80.6
5.0 g/L	233.9	0.18	3.780	84.6

Table 4. Corrosion parameters obtained by impedance measurements for mild steel in 0.5M HCl at various concentrations of Lippia Alba oil.

Inhibitor concentration	R_{ct} (ohm.cm ²)	f_{max} (Hz)	C_{dl} (mF/cm ²)	E (%)
0.5M HCl	36.1	0.35	12.246	-
1.0 g/L	124.7	0.23	5.549	71.1
4.0 g/L	182.1	0.21	4.161	80.2
5.0 g/L	271.2	0.17	3.452	86.7

The electrochemical impedance diagrams indicate two significant effects in absence and presence of the Eucalyptus and Lippia Alba essential oils: the charge transfer resistance significantly increases, and the f_{max} decreases, in the presence of the essential oil, decreasing the capacitance value, which may be caused by reduction in the local dielectric constant and/or by an increase in the thickness of the electrical double-layer. These results show that the presence of the essential oils modifies the electric double-layer structure suggesting that the inhibitor molecules act by adsorption at the metal/solution interface. Furthermore, C_{dl} decreases with increase of the concentration of inhibitor. This phenomenon is generally related to the adsorption of organic molecules on the metal surface and then leads to a decrease in the dielectric constant and/or an increase in the thickness of the electrical double layer (37,38):

$$C_{dl} = \frac{\epsilon_o \epsilon S}{d} \quad (2)$$

Where δ is the thickness of the protective layer, S is the electrode area, ϵ_o the vacuum permittivity and ϵ is dielectric constant of the medium.

For other part, a low capacitance may result if water molecules at the electrode interface are largely replaced by organic inhibitor molecules through adsorption. The larger inhibitor molecules also reduce the capacitance through the increase in the double layer thickness (39,40). Deviations from a perfect circular shape indicate frequency dispersion of interfacial impedance. This anomalous phenomenon is attributed in the literature to the non homogeneity of the electrode surface arising from the surface roughness or interfacial phenomena (41-43). The charge transfer resistance (R_{ct}) values were calculated from the difference in impedances at lower and higher frequencies. The double layer capacitance (C_{dl}) was calculated from the following equation:

$$C_{dl} = \frac{1}{2\pi f_{max} R_{ct}} \quad (3)$$

Where f_{max} is the maximum frequency at which the imaginary component of the impedance is maximal. From Table 3 and 4, it is clear that the R_{ct} values increased and that the C_{dl} values decreased with increasing inhibitor concentration. These results indicate a decrease in the active surface area caused by the adsorption of the inhibitors on the mild steel surface, and it suggests that the corrosion process became hindered. The best result for the inhibition efficiency of these essential oils were obtained at a concentration of 5.0 g/L, with efficiency equal to 84.6% and 86.7% for Eucalyptus and Lippia Alba oil, respectively.

3.3. Tafel polarization curves

Polarization curves for mild steel in presence and absence of different concentrations of Eucalyptus and Lippia Alba essential oils in non aerated solutions are shown in Figure 3 and 4. The extrapolation of Tafel straight line allowed the calculation of the corrosion current density (I_{corr}). The values of I_{corr} , the corrosion potential (E_{corr}), cathodic Tafel slope (β_c), and inhibition efficiency (E %) are given in Table 5 and 6 for Eucalyptus and Lippia Alba oil respectively. The (E %) was calculated using the following equation (44):

$$E(\%) = \frac{I_{corr}^o - I_{corr}}{I_{corr}^o} \times 100 \quad (4)$$

where I_{corr}° and I_{corr} are uninhibited and inhibited corrosion current densities, respectively. Under the experimental conditions performed, the cathodic branch represents the hydrogen evolution reaction, while the anodic branch represents the iron dissolution reaction. Some of the authors proposed the following mechanism for the corrosion of iron and steel in acid solution (45,46):



The cathodic hydrogen evolution:

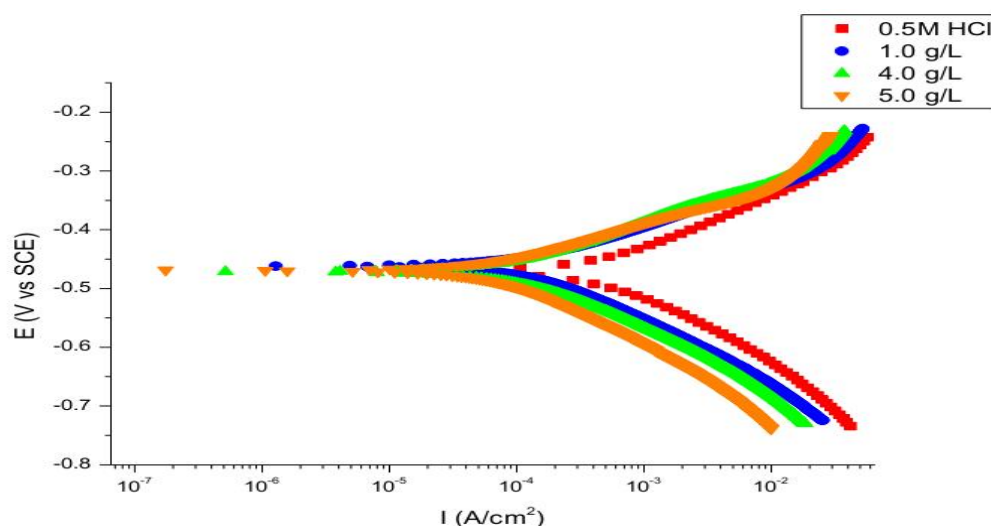
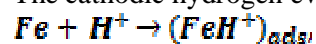


Figure 3. Tafel polarization curves in 0.5M HCl with and without Eucalyptus oil at different concentrations

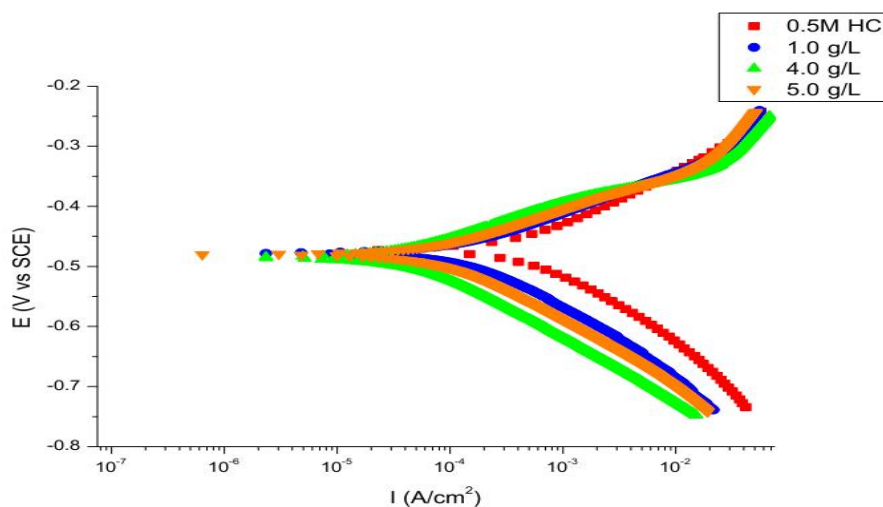


Figure 4. Tafel polarization curves in 0.5M HCl with and without Lippia Alba oil at different concentrations

Table 5. Electrochemical parameters of mild steel at various concentrations of Eucalyptus oil in 0.5M HCl

Inhibitor concentration	-E _{Corr} (V)	β _C (V/dec)	I _{Corr} (mA/cm ²)	E (%)
0.5M HCl	0.47	0.11	1.102	-
1.0 g/L	0.46	0.10	0.227	79.5
4.0 g/L	0.47	0.15	0.137	87.3
5.0 g/L	0.47	0.12	0.089	91.1

Table 6. Electrochemical parameters of mild steel at various concentrations of Lippia Alba oil in 0.5M HCl

Inhibitor concentration	-E _{Corr} (V)	β _C (V/dec)	I _{Corr} (mA/cm ²)	E (%)
0.5M HCl	0.47	0.14	1.102	-
1.0 g/L	0.48	0.11	0.198	82.1
4.0 g/L	0.48	0.15	0.138	87.4
5.0 g/L	0.49	0.18	0.093	92.6

Inspection of these results reveal that in presence of inhibitors, the value of corrosion density (I_{corr}) was decreased. This behavior reflects its ability to inhibit the corrosion of mild steel in 0.5M HCl solution. Both the anodic and cathodic current densities were decreased in figure 3 and 4, indicating that Eucalyptus and Lippia Alba essential oils suppressed both the anodic and cathodic reactions through adsorption on the mild steel surface. This suggests that the essential oils act as mixed type corrosion inhibitor for mild steel in 0.5M HCl solution. Generally, the modes of the inhibition effect of inhibitors are classified into three categories (47-48): geometric blocking effect of adsorbed inhibitive species, active sites blocking effect by adsorbed inhibitive species, and electrocatalytic effect of the inhibitor or its reaction products. It has been discussed in the case of the first mode that inhibition effect comes from the reduction of the reaction area on the surface of the corroding metal, whereas for the other two modes the inhibition effects are due to the changes in the average activation energy barriers of the anodic and cathodic reactions of the corrosion process. The cathodic Tafel slope (β_c) show slight changes with the addition of Eucalyptus and Lippia Alba, which suggests that the inhibiting action occurred by simple blocking of the available cathodic sites on the metal surface, which lead to a decrease in the exposed area necessary for hydrogen evolution and lowered the dissolution rate with increasing essential oils concentration (table 5 and 6). The parallel cathodic Tafel plots obtained in Figure 3 and 4 indicate that the hydrogen evolution is activation controlled and the reduction mechanism is not affected by the presence of inhibitor (48).

3.4. Weight loss measurements

3.4.1. Effect of temperature

In order to study the effect of temperature on the inhibition efficiencies of Eucalyptus and Lippia Alba essential oils, weight loss measurements were carried at three temperature values: 298 , 333 and 383 K and during 4 hours of immersion in absence and presence of inhibitors at optimum concentration (5.0 g/L) determined in electrochemical measurements. The various corrosion parameters obtained are listed in Table 7 for essential oils studied. Figure 5 illustrates the variation of corrosion rate in the absence and of inhibitor at optimum concentration at different temperatures. From the weight loss results, the corrosion rate (CR), the inhibition efficiency (E%) of inhibitors and degree of surface coverage (Θ) were calculated using equations 5, 6 and 7 (49):

$$CR = \left(\frac{\Delta W}{Sxt} \right) \quad (5)$$

$$E(\%) = \left(1 - \frac{W_{corr}}{W_{corr}^o} \right) \times 100 \quad (6)$$

$$q = \left(1 - \frac{W_{corr}}{W_{corr}^o}\right) \quad (7)$$

Where W_{corr} and W_{corr}^o are the weight losses for mild steel in the presence and absence of the essential oils in HCl solution and Θ is the degree of surface coverage of the inhibitors. ΔW is the difference of weight loss for mild steel with and without inhibitors, S is the exposure area of the metallic specimens and t is the immersion time of the metal in corrosive solution.

Table 7. Corrosion parameters for mild steel in 0.5M HCl in absence and presence of optimum concentration of essential oils at different temperatures

Temperature (K)	Inhibitor	CR(mg/cm ² .h)	Θ	E (%)
298	0.5M HCl	13.64	-	-
	Eucalyptus	1.09	0.92	92
	Lippia Alba	1.25	0.90	90
333	0.5M HCl	25.68	-	-
	Eucalyptus	6.93	0.73	73
	Lippia Alba	6.74	0.74	74
383	0.5M HCl	31.50	-	-
	Eucalyptus	9.40	0.70	70
	Lippia Alba	9.81	0.69	69

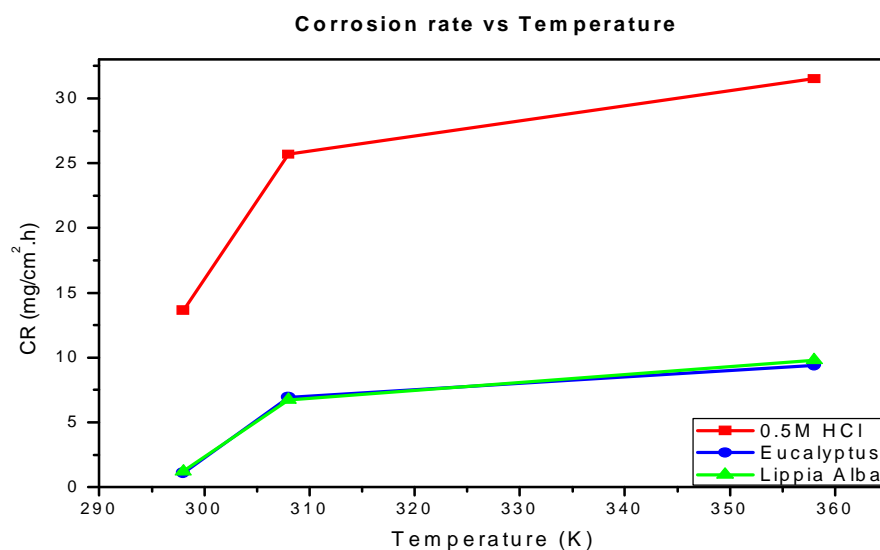


Figure 5. Variation of CR in 0.5M HCl on steel surface without and with of optimum concentration of essential oil at different temperatures.

The fractional surface coverage (Θ) can be easily determined from the weight loss measurements by the ratio $E\% / 100$, where $E\%$ is inhibition efficiency and calculated using equation 6. The data obtained suggest that essential oils get adsorbed on the steel surface at all temperatures studied and corrosion rates increased in absence and presence of inhibitor with increase in temperature in 0.5M HCl solutions. In acidic media, corrosion of metal is generally accompanied with evolution of H_2 gas; rise in temperature usually accelerates the corrosion reactions which results in higher dissolution rate of the metal. Inspection of Table 7 showed that corrosion rate increased with increasing temperature both in uninhibited and inhibited solutions while the inhibition efficiency of essential oils decreased with temperature. A decrease in inhibition efficiencies with the increase temperature in presence of essential oils might be due to weakening of physical adsorption. In order to calculate activation parameters for the corrosion process, Arrhenius equation (8) and transition state equation (9) were used (50):

$$CR = A \exp\left(\frac{-E_a}{R \times T}\right) \quad (8)$$

$$CR = \frac{R \times T}{N \times h} \exp\left(\frac{-\Delta S_a}{R}\right) \exp\left(\frac{-\Delta H_a}{R \times T}\right) \quad (9)$$

where CR is the corrosion rate, R the gas constant, T the absolute temperature, A the pre-exponential factor, h the Plank's constant and N is Avogrado's number, E_a the activation energy for corrosion process, ΔH_a the enthalpy of activation and ΔS_a the entropy of activation. The apparent activation energie (E_a) at optimum concentration of essential oils was determined by linear regression between Ln CR and 1/T (Figure 6) and the result is shown in Table 8.

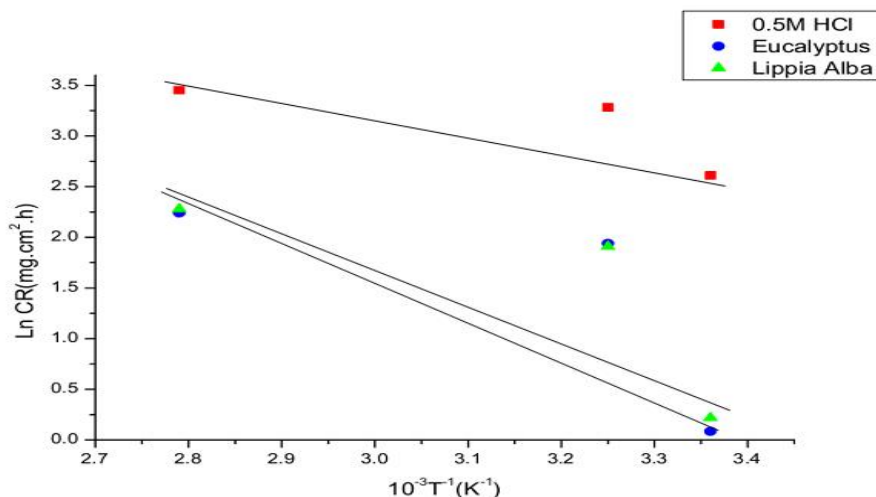


Figure 6. Arrhenius plots of log CR vs. 1/T for mild steel in 0.5M HCl in the absence and the presence of essential oils at optimum concentration (5.0 g/L).

Table 8. Activation parameters E_a , ΔH_a and ΔS_a for the mild steel dissolution in 0.5M HCl in the absence and the presence of essential oils at optimum concentration.

Inhibitor	E_a (kJ/mol)	ΔH_a (KJ/mol)	ΔS_a (J/mol.K)
0.5M HCl	9.33	7.20	-143.85
Eucalyptus	23.86	21.75	-114.45
Lippia Alba	22.85	20.35	-117.06

Inspection of Table 8 showed that the value of E_a determined in 0.5M HCl containing essential oils is higher (**23.86 and 22.85 kJ/mol** for Eucalyptus and Lippia Alba essential oils, respectively) than that for uninhibited solution (**9.34 kJ/ mol**). The increase in the apparent activation energy may be interpreted as physical adsorption that occurs in the first stage. The increase in activation energy could be attributed to an appreciable decrease in the adsorption of the inhibitor on the steel surface with increase in temperature. As adsorption decreases more desorption of inhibitor occur because these two opposite processes are in equilibrium. Due to more desorption of inhibitor molecules at higher temperatures the greater surface area of steel comes in contact with aggressive environment, resulting increased corrosion rates with increase in temperature (51).

Figure 7 showed a plot of Ln (CR/T) versus 1/T. The straight lines are obtained with a slope ($\Delta H_a/R$) and an intercept of ($\text{Ln } R/Nh + \Delta S_a/R$) from which the values of the values of the values of ΔH_a and ΔS_a are calculated for each essential oil analyzed and are given in Table 8. Inspection of these data revealed that the thermodynamic parameter (ΔH_a) for dissolution reaction of steel in 0.5M HCl in the presence of essential oils is higher (**21.75 and 20.35 kJ/mol** for Eucalyptus and Lippia Alba essential oils, respectively) than that of in the absence of inhibitors (**7.20 kJ/ mol**). The positive sign of ΔH_a reflect the endothermic nature of the steel dissolution process suggesting that the dissolution of steel is slow (52) in the presence of inhibitor. Large and negative

value of entropie (ΔS_a) imply that the activated complex in the rate determining step represents an association rather than a dissociation step, meaning that a decrease in disordering takes place on going from reactant to the activated complex.

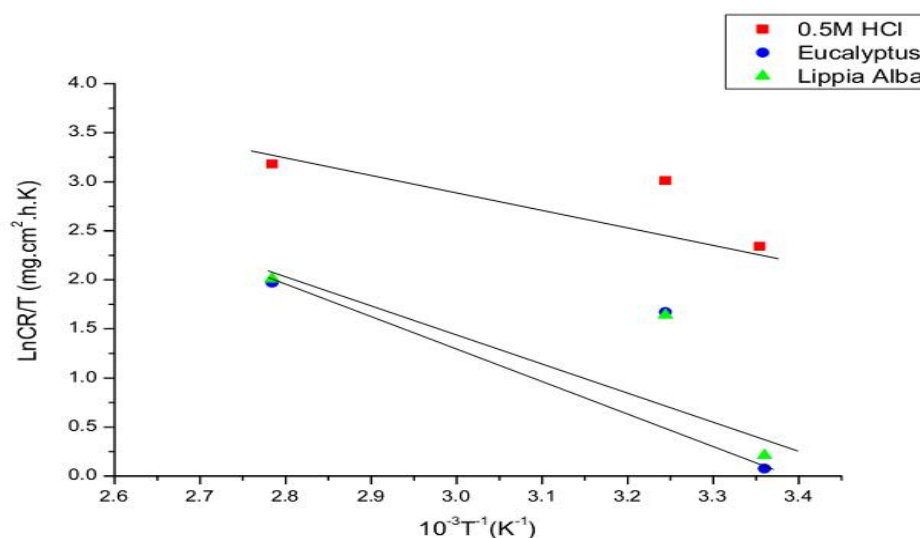


Figure 7. Arrhenius plots of $\ln CR/T$ vs. $1/T$ for steel in 0.5M HCl in the absence and the presence of essential oils at optimum concentration (5.0 g/L).

3.5. Fourier Transform Infrared Spectroscopy (FTIR)

In present study, FTIR spectra were used to support the fact that the corrosion inhibition of mild steel in acid media is due to in part, at the adsorption of inhibitor molecules on the surface of material (53,54). The IR spectra of Eucalyptus and Lippia Alba essential oils as inhibitor layers (Figure 8 and 9), and their predominant peaks and respective wavelength values (Table 9 and 10) are shown below. Since essential oils contained organic compounds and these organic compounds were adsorbed on the metal surface providing protection against corrosion. So, FTIR analyses of metal surface can be useful for predicting whether organic inhibitors are adsorbed or not adsorbed on the metal surface. In present study, FTIR spectra were used to support the fact that corrosion inhibition of mild steel in acid media is due to the adsorption of inhibitor molecules on the mild steel surface. Here, it were also observed the IR spectra of concentrated essential oils studied (Figure 10 and 11) with their predominant peaks and respective wavelength values (Table 11 and 12) (55,56). We conclude that FTIR spectra support good inhibition performance of Eucalyptus and Lippia Alba oil for mild steel corrosion in hydrochloric acid solution.

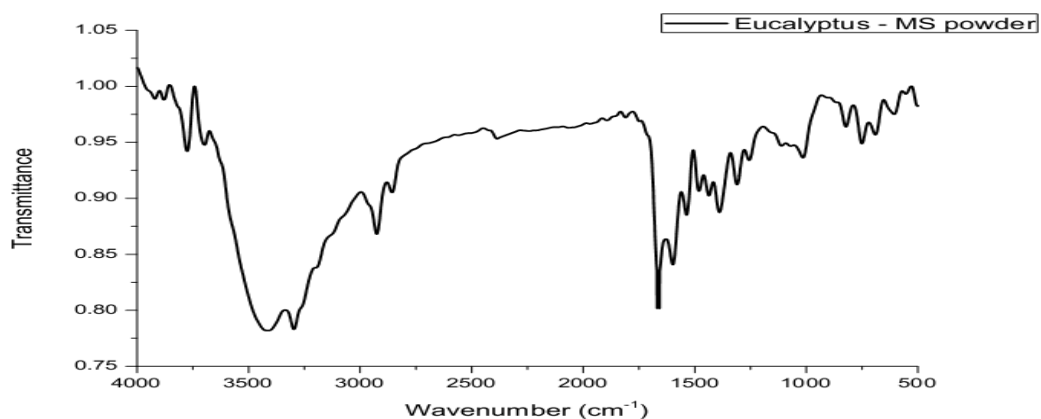


Figure 8. IR spectra of the product between Eucalyptus oil and MS powder specimen

Table 9. IR peaks for Eucalyptus oil and MS powder specimen

Wave number (cm ⁻¹)	Vibration mode	Intensity
3416.27	O-H stretching	High
2925.60	(-CH ₂) asymmetric stretching	Low
1629.84	C=O stretching (ketone carbonyl)	Medium
1385.23	(-CH ₃) asymmetric deformation	Low
1054.37	C-O stretching	Low
1029.62	O-H in plane bending	Low

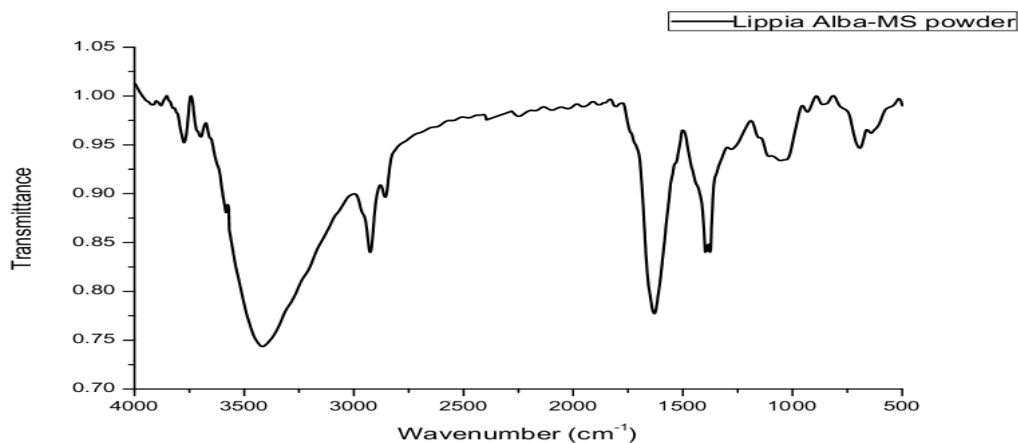


Figure 9. IR spectra of the product between Lippia Alba oil and MS powder specimen

Table 10. IR peaks for Lippia Alba oil and MS powder specimen

Wave number (cm ⁻¹)	Vibration mode	Intensity
3411.01	O-H stretching	High
2925.51	(-CH ₂) asymmetric stretching	Low
1663.90	C=O stretching (aldehyde carbonyl)	Medium
1462.98	(-CH ₂) asymmetric deformation	Low
1389.49	(-CH ₃) asymmetric deformation	Low
1055.05	C-O stretching	Low
1030.23	O-H in plane bending	Low

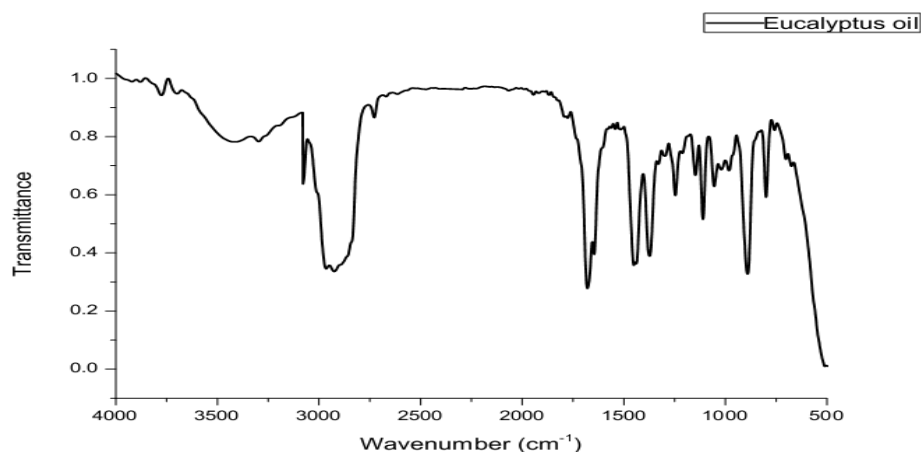


Figure 10. IR spectra of Eucalyptus oil

Table 11. IR peaks for Eucalyptus oil

Wave number (cm ⁻¹)	Vibration mode	Intensity
3525.15	O-H stretching	Low
2925.20	(-CH ₂) asymmetric stretching	Medium
1679.28	C=O stretching (aldehyde carbonyl)	High
1450.73	(-CH ₃) asymmetric deformation	Medium
1372.68	(-CH ₃) symmetric deformation	Medium
1055.39	C-O stretching	Low
1030.65	O-H in plane bending	Low

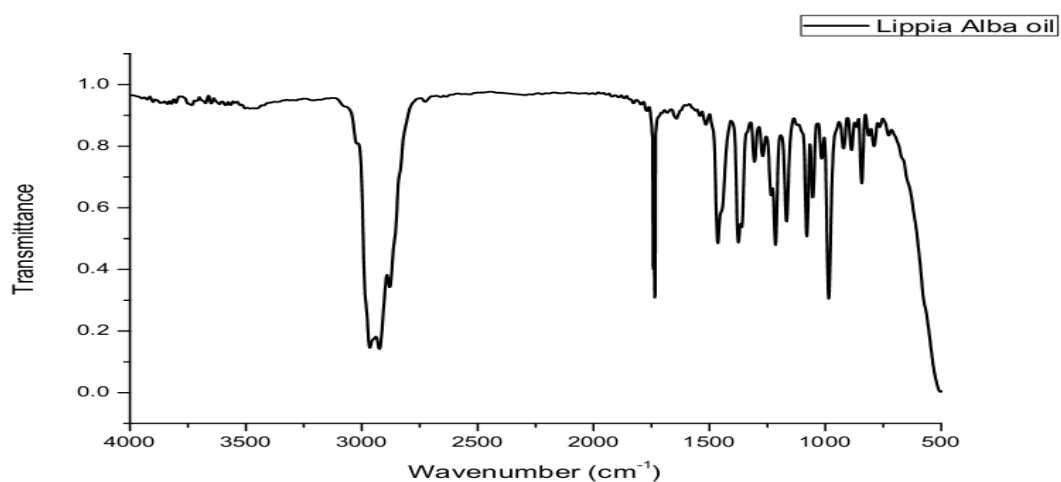


Figure 11. IR spectra of Lippia Alba oil

Table 12. IR peaks for Lippia Alba oil

Wave number (cm ⁻¹)	Vibration mode	Intensity
2923.83	(-CH ₂) asymmetric stretching	High
1739.77	C=O stretching (ketone carbonyl)	High
1464.11	(-CH ₂) asymmetric deformation	Medium
1375.67	(-CH ₃) asymmetric deformation	Medium
1167.55	(-CH ₂) symmetric deformation	Medium
1054.37	C-O stretching	Low
1029.43	O-H in plane bending	Low

3.6. Mechanism of inhibition for mild steel in HCl solution

FTIR showed that the essential oils contains oxygen atoms in functional groups (O-H, C = O, C-H, C-O) and insaturations (C = C), which meets the general consideration of typical corrosion inhibitors. The nonbonded electrons of heteroatoms get protonated and thereby they get adsorbed on the negatively charged metal surface. Due to electrostatic interaction, the protonated constituent's molecules are adsorbed (physisorption) and high inhibition is expected. Eucalyptus and Lippia Alba oil molecules (Figure 12 and 13) can also adsorb on the metal surface on the basis of donor-acceptor interactions between π -electrons of aromatic ring and vacant d-orbitals of Fe. When protonated Eucalyptus and Lippia Alba essential oil molecules adsorbed on metal surface, coordinate bond maybe formed by partial transference of electrons from the polar atoms (O atoms) to the metal surface. This assumption could be further confirmed by the FTIR results that Eucalyptus and Lippia Alba oil could adsorb onto steel surface to form a dense and more tightly protective film covering both cathodic and anodic reaction sites and, thus, retarding corrosion phenomenon (57).

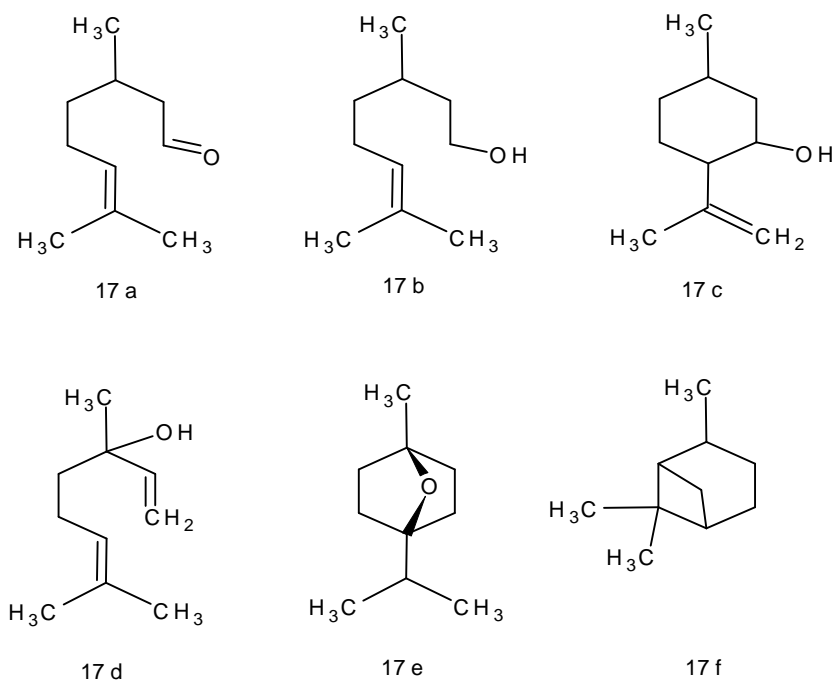


Figure 12. Eucalyptus oil molecules: 17a-Citronellal, 17b-Citronellol, 17c-Isopulegol, 17d-linalool, 17e-1,8-Cineole and 17f- β-pinene

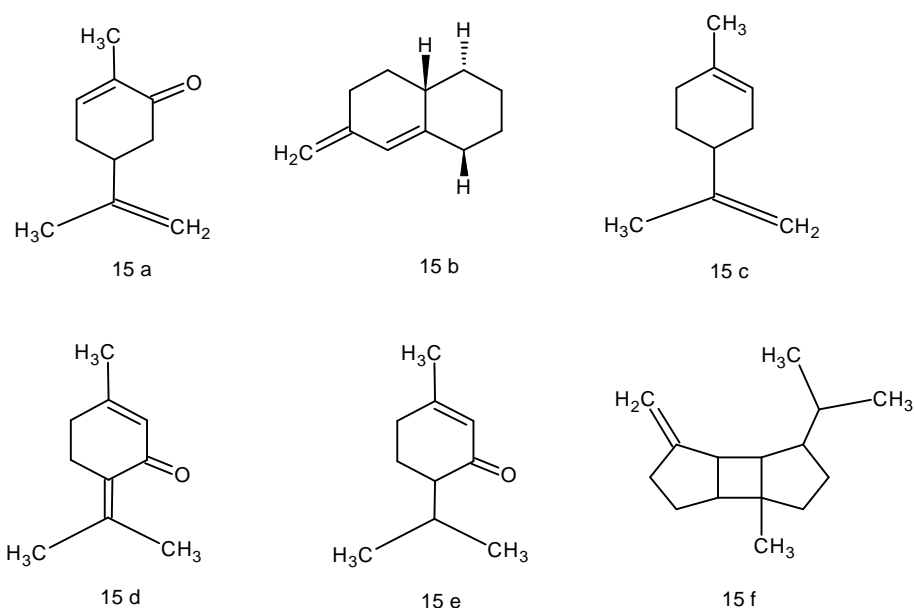


Figure 13. Lippia Alba oil molecules: 15a-Carvona, 15b-Biclosquifelandrene, 15c-limonene, 15d-Piperitenone, 15e-Piperitone and 15f- β-Bourbonene

3.7. Optical microscopy

To evaluate the surface morphology of mild steel, optical microscopy photographs were recorded for MS specimens exposed to test solution with and without essential oils (5.0 g/L) at a resolution of 100 x (10 μ m). The optical photographs are given in figures 14, 15, 16 and 17. The mild steel sample immersed in the inhibitor solutions has apparently smooth surface when compared with that of corroded rough of specimen immersed in HCl alone. This is due to the adsorption of inhibitor molecules on the metal surface forming a protective layer, decrease the material degradation. (58).

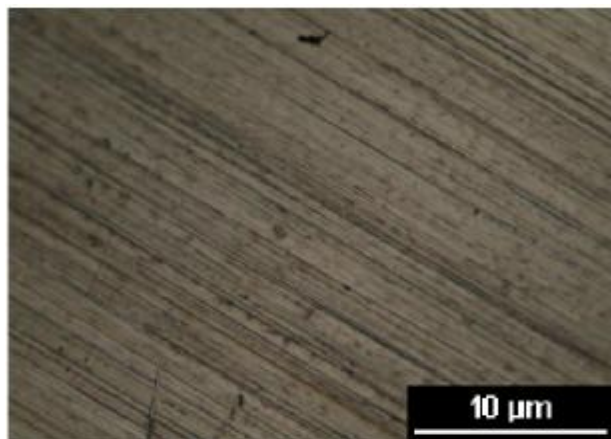


Figure 14. Polished mild steel surface sample

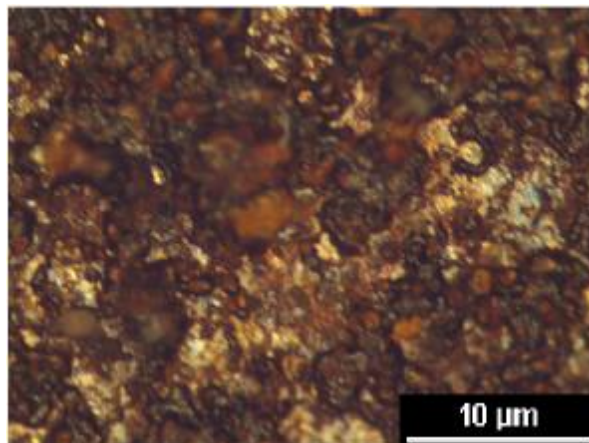


Figure 15. Mild steel surface sample exposed to 0.5M HCl without inhibitors

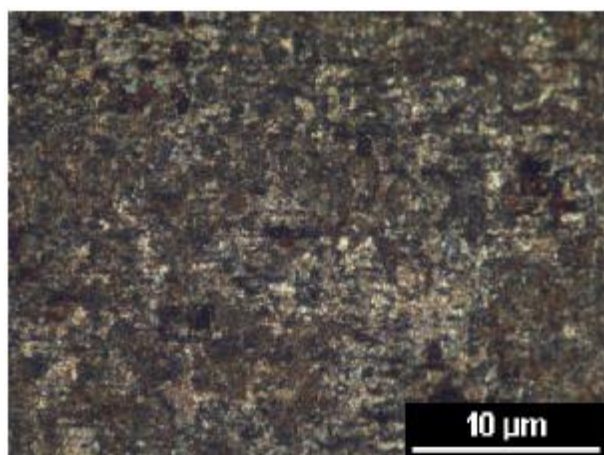


Figure 16. Mild steel surface sample exposed to 0.5M HCl with 5.0 g/L Eucalyptus oil

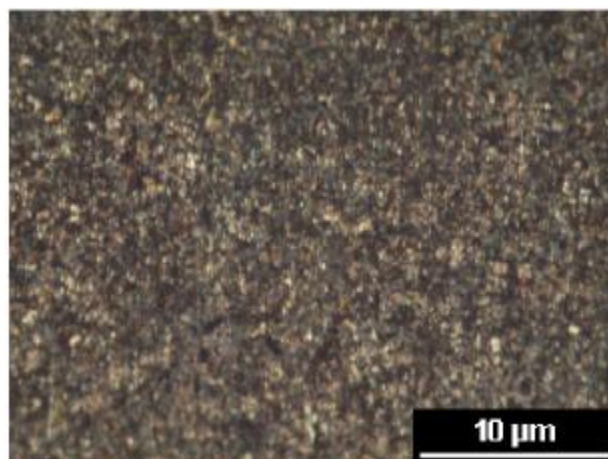


Figure 17. Mild steel surface sample exposed to 0.5M HCl with 5.0 g/L Lippia Alba oil

4. Conclusions

1. Results obtained through weight loss measurements and electrochemical tests demonstrated that the Eucalyptus and Lippia Alba essential oils act as efficient corrosion inhibitors of the mild steel in 0.5 M HCl solution.
2. The corrosion process was inhibited by adsorption of the organic matter on the mild steel surface.
3. Inhibition efficiency increases with increase in the concentration of the Eucalyptus and Lippia Alba essential oils but decreases with rise in temperature.
4. The decrease in the charge transfer resistance and double layer capacitance values, with the increase in the inhibitor concentration, showed that essential oils formed protective layers on the mild steel surface, covering areas where HCl solution degrades and corrodes rapidly.
5. Tafel polarization measurements show that Eucalyptus and Lippia Alba act essentially as a mixed type inhibitor.
6. The physic adsorption of the inhibitor on the surface of the mild steel is mainly credited to the oxygen atoms and insaturations (C=C) present in the essential oil molecules, obtaining the formation of the film on the metal/acid solution interface, decreasing the degradation of the material.

Acknowledgements

This research was supported financially by Centro de Investigaciones en Corrosion (GIC), furthermore to provide the apparatus for the performance of different electrochemical techniques and extend the laboratory facilities.

References

1. Bouyanzer, A.; Majidi, L.; Hammouti, B. *Bull. Electrochem.* 22 (2006) 321-324.
2. Chebabe, D.; Ait Chikh, Z.; Hajjaji, N. *Corros. Sci.* 45 (2003) 309-320.
3. Quraishi, M. A.; Singh, A.; Singh, V. K.; Yadav, *Mater. Chem. Phys.* 122 (2010) 114-122.
4. Boris M.; Miksin, Alla.; Furman, Y.; Margarita, A.; *Abstracts, NACE International Corrosion Conference & Expo*, Atlanta, Georgia, 2009.
5. Orubite, K.O. ; Oforka, N.C.; *Mater. Letters.* 58 (2004) 1768.
6. Khedr, M. G. A. ; Lashien, A. M. S. *Corros. Sci.* 33 (1992) 137-151.
7. Chauhan, L.R.; Gunasekaran, G.; *Corros. Sci.* 49 (2007) 1143.
8. Noor, E.A. *J. Eng. Appl. Sci.* 3 (2008) 23-30.
9. Buchweishajja, J.; M hinzi, G. S. *Port. Electrochem. Acta* 23 (2008) 257-265.
10. Oguzie, E. E. *Corros. Sci.* 50 (2008) 2993-2998.
11. Okafor, P. C. ; Ikpi, M. E.; Uwah, I. E.; E benso, E.E.; Ekpe, U. J. *Corros. Sci.* 50 (2008) 2310-2317.
12. Badiea, A. M.; Mohana, K. N. *J. Mater. Eng. Perform.* 18 (2009) 1264-1271.
13. A El-Etre, A. Y.; Abdallah, M.; El-Tantawy, Z. E. *Corros. Sci.* 47 (2005) 385-395.
14. Kliškić M., Radošević J., Gudić S., Katalinić V.; *J. Appl. Electrochem.* 30 (2000) 823-830.
15. Lebrini, M.; Robert, F.; Roose, C. *Int. J. Electrochem. Sci.* 5 (2010) 1698 - 1712.
16. Verma, A.S.; Mehta, G.N.; *Bull. Electrochem.* 15 (1999) 67.
17. Loto, C. A.; Loto, R.T. *Int. J. Electrochem. Sci.* 6 (2011) 4900 - 4914.
18. Okafor, P. C.; E benso, Eno E.; Udofot J. E. *Int. J. Electrochem. Sci.* 5 (2010) 978 - 993.
19. Oguzie, E. E.; *Corros. Sci.* 50 (2008) 2993-2998.
20. Fresia Chandía, C.; Hernández H, Sergio.; *Cienc. Ahora* 24 (2009) 52-55.
21. Gomma, G. K.; Wahdan, M. H.; *Ind. J. Chem. Technol.* 2 (1995) 107.
22. Ashassi-Sorkhabi, H.; Seifzadeh, D.; Hosseini, M. G.; *Corrosion Sci.* 50 (2008) 3363-3370.
23. Hefner, A.; G.T.; North, N.A.; Tan, S.H.; *J. Sci. Eng.* 32 (1997) 657-667.
24. Chetouani, M. Daoudi, B. Hammouti, T. Ben Hadda; Benkaddour, M. *Corros. Sci.* 48 (2006) 2987.
25. Tebbji, K.; Hammouti, B.; Oudda, H.; Ramdani, A.; Benkadour, M.; *Appl. Surf. Sci.* 252 (2005) 1378-1385.
26. El-Sanabary, A.; Badran, B.; M.El-Sawy, S.; *J. Appl. Sci. Res.* 10 (2008) 1149-1154.
27. Nnanna, L. A.; Onwuagba, B. N.; Mejeha, I. M.; Okeoama, K. B.; *African J. P. Appl. Chem.* 4 (2010) 011-016.
28. Herrag, L.; Chetouani, A.; Elkadiri, S.; Hammouti, B.; Aouniti, A. *Port. Electrochim. Acta* 26 (2008) 211-220.
29. Adhikari, V.; Saliyan, V. R. *Indian. J. Chem. Technol.* 16 (2009) 162.
30. Luo, H.; Guan, Y.C.; Han, K.N.; *J. Sci. Eng.* 27 (1998) 619-627.
31. Benabdellah, M.; Benkaddour, M.; Hammouti, B.; Bendahhou, M.; Aouniti, A.; *Appl. Surf. Sci.* 252 (2006) 6212-6217.
32. Hosseini, M.; Mertens, S.; Ghorbani, M.; Arshadi, M.R.; *Mater. Chem. and Phys.* 78 (2003) 800-808.
33. Mahdavian, M.; Attar, M. M.; *Corros. Sci.* 48 (2006) 4152.
34. Antonijevic, M.M.; Petrovic, M.; *Corros. Sci.* 51 (2009) 28-34.
35. Geler, E.; Azambuja, D.S. *Corros. Sci.* 42 (2000) 631.
36. Schorr, M.; Yahalom, J.; *J. Corrosion Sci.* 12 (1972) 867-868.

37. International, N.; *Crude Unit Distillation Column Overhead Corrosion*, ed., NACE International publications: Houston, 2008.
38. Sherif El-S.M.; Erasmus, R.M.; Comins, J.D. *J. Coll. Inter. Sci.* 311 (2007) 144.
39. J.O'M. Bochriss, A.K.N. Reddy, *Modern. Electrochemistry*, vol. 2, Plenum Press, New York, 1977, pp. 1267.
40. Dehri, I.; Ozcan, M.; *Mater. Chem. Phys.* 98 (2006) 316.
41. Peña, Darío Y.; Rocío, S.; Vásquez, C. *Artíc. Científ. Ing. Desarrol.* 27 (2010) 1-28
42. Prabhu, R.A.; Shanbhag, A.V.; Venkatesha, T.V. *J. Appl. Electrochem.* 37 (2007) 491–497.
43. Anand, R.R.; Hurd, R.M.; Hackerman, N. *J. Electrochem. Soc.* 112 (1965) 138–144.
44. Bouyanzer, A.; Hammouti, B.; Majidi, L.; *Mater. Letters* 60 (2006) 2840.
45. Ruiz Díaz E.; Becerra, E.; Gualdrón, A.; Villareal, Y.; Cañas, D.; *Estandarización de la prueba para evaluación de potencial de HCI*, ed., Instituto Colombiano del petróleo: Bucaramanga, 2009.
46. Salih, S.; Al-Juaid; *Port. Electrochim. Acta* 23 (2007) 365- 367.
47. Sánchez, M.; *Doctoral thesis*, Universidad de los Andes, Venezuela, 2004.
48. Muralidharan, S.; Quraishi, M. A.; Iyer, V. K. *Corrosion Sci.* 37 (1995) 1739–1750.
49. Thompson, J.R.; Scheetz, E.; Schock, R.; Lytl A.; Delaney, J.; *Abstracts, Water Quality Technology Conference*, Denver, 1997.
50. Popova, A. *Corros. Sci.* 49 (2007) 2144.
51. Martinez, S.; Stern, I. *Appl. Surf. Sci.* 199 (2002) 83.
52. Znini, M.; Bouklah, M.; Kharchouf, S.; Majidi, L.; Aouniti, A.; Hammouti, A.; Bouyanzer, B.; *Int. J. Electrochem. Sci.* 6 (2011) 691 – 704.
53. Xometl, O.; Zamudio R.; López, J. M.; *Doctotal thesis*, Instituto Politécnico Nacional, Escuela Superior de Ingeniería Química e Industrias Extractivas., México D.F, 2005.
54. Thusnavis, G.; Narayanan, R.; Sankara, M.; Kumar, K.P.; *J. Mater. Environ. Sci.* 2 (2010) 119- 128.
55. Zaafarany, M.; Abdallah, J.; *J. Electrochem. Sci.* 5 (2010) 19-22.
56. Durnie, W., De Marco, R., Kinsella, B., Jefferson, A. *J. Electrochem. Soc.* 146 (1999) 1751.
57. Soltani, N.; Behpour, M.; Ghoreishi, S M.; Naeimi, H. *Corros. Sci.* 52 (2010) 1351– 1361.
58. Gopi, D.; Manimozhi, S.; Govindaraju, K. M.; Manisankar, P.; Rajeswari, S.; *J. Appl. Electrochem.* 37 (2007) 439-449.

(2013) <http://www.jmaterenvirosci.com>